EUROPEAN SOCIETY OF RADIOLOGY
European Radiology

INTERVENTIONAL

Ablative margin quantification using deformable versus rigid image registration in colorectal liver metastasis thermal ablation: a retrospective single-center study

Yuan-Mao Lin[1], Iwan Paolucci[1], Jessica Albuquerque Marques Silva[1], Caleb S. O'Connor[2], Jun Hong[2], Ketan Y. Shah[1], Mohamed E. Abdelsalam[1], Peiman Habibollahi[1], Kyle A. Jones[2], Kristy K. Brock[2] and Bruno C. Odisio[1]*

Abstract

Purpose To investigate the correlation of minimal ablative margin (MAM) quantification using biomechanical deformable (DIR) versus intensity-based rigid image registration (RIR) with local outcomes following colorectal liver metastasis (CLM) thermal ablation.

Methods This retrospective single-institution study included consecutive patients undergoing thermal ablation between May 2016 and October 2021. Patients who did not have intraprocedural pre- and post-ablation contrast-enhanced CT images for MAM quantification or follow-up period less than 1 year without residual tumor or local tumor progression (LTP) were excluded. DIR and RIR methods were used to quantify the MAM. The registration accuracy was compared using Dice similarity coefficient (DSC). Area under the receiver operating characteristic curve (AUC) was used to test MAM in predicting local tumor outcomes.

Results A total of 72 patients (mean age 57; 44 men) with 139 tumors (mean diameter 1.5 cm ± 0.8 (SD)) were included. During a median follow-up of 29.4 months, there was one residual unablated tumor and the LTP rate was 17% (24/138). The ranges of DSC were 0.96–0.98 and 0.67–0.98 for DIR and RIR, respectively ($p < 0.001$). When using DIR, 27 (19%) tumors were partially or totally registered outside the liver, compared to 46 (33%) with RIR. Using DIR versus RIR, the corresponding median MAM was 4.7 mm versus 4.0 mm, respectively ($p = 0.5$). The AUC in predicting residual tumor and 1-year LTP for DIR versus RIR was 0.89 versus 0.72, respectively ($p < 0.001$).

Conclusion Ablative margin quantified on intra-procedural CT imaging using DIR method outperformed RIR for predicting local outcomes of CLM thermal ablation.

Clinical relevance statement The study supports the role of biomechanical deformable image registration as the preferred image registration method over rigid image registration for quantifying minimal ablative margins using intraprocedural contrast-enhanced CT images.

---

*Correspondence:
Bruno C. Odisio
bcodisio@mdanderson.org
Full list of author information is available at the end of the article

🖄 Springer

Key Points

• *Accurate and reproducible image registration is a prerequisite for clinical application of image-based ablation confirmation methods.*

• *When compared to intensity-based rigid image registration, biomechanical deformable image registration for minimal ablative margin quantification was more accurate for liver registration using intraprocedural contrast-enhanced CT images.*

• *Biomechanical deformable image registration outperformed intensity-based rigid image registration for predicting local tumor outcomes following colorectal liver metastasis thermal ablation.*

Keywords Ablation techniques, Colorectal neoplasms, Computed tomography (image processing), computer assisted, Liver

Introduction

Colorectal cancer ranks as the second leading cause of cancer-related deaths worldwide. During the progression of the disease, around 30% of colorectal cancer patients develop colorectal cancer liver metastasis (CLM) [1, 2]. In recent decades, thermal ablation has been incorporated into treatment guidelines as a viable alternative to surgery for selected patients with oligometastatic disease [3]. Thermal ablation offers several key advantages. Firstly, its tissue-sparing nature allows precise targeting of tumors while minimizing damage to the surrounding liver tissue, improving ability to offer salvage therapies at the time of intrahepatic recurrence. Additionally, it can be performed using a minimally invasive percutaneous approach, reducing treatment-related complications, hospitalization time, and healthcare-related costs [4]. Collectively, such characteristics contribute to a significant reduction in morbidity associated with treatment and enhance the overall efficacy of managing CLM [5].

When considering oncological local outcomes, numerous observational studies indicate that achieving ablation margins larger than 5 mm is deemed the most crucial technical factor for ensuring effective local tumor control [6–9]. Despite the improved accuracy of three-dimensional measurements facilitated by ablation confirmation software packages, the current available methods for assessing ablation margins are highly variable. Most of the existing three-dimensional techniques available for clinical use rely on either rigid image registration (RIR) or intensity-based deformable image registration (DIR) [7, 9]. However, both of these techniques are susceptible to registration errors resulting from liver deformity caused by patient positioning and breathing, placement of the ablation applicator, hydrodissection, and tissue contraction associated with the ablation process. A recent study has proposed a biomechanical DIR method to address deformations for quantifying ablative margins, which has been validated in a retrospective cohort [6, 10]. However, there is a lack of studies comparing different image registration methods in terms of local tumor outcomes. This gap in research may contribute to misinterpretation on the utility of different ablation confirmation methodologies, ultimately resulting in hesitancy to its broader application.

The objective of this study was to compare the predictive performance of minimal ablative margins (MAMs) quantified by biomechanical deformable image registration (DIR) and intensity-based rigid image registration (RIR) methods for predicting local tumor outcomes following colorectal liver metastasis (CLM) thermal ablation.
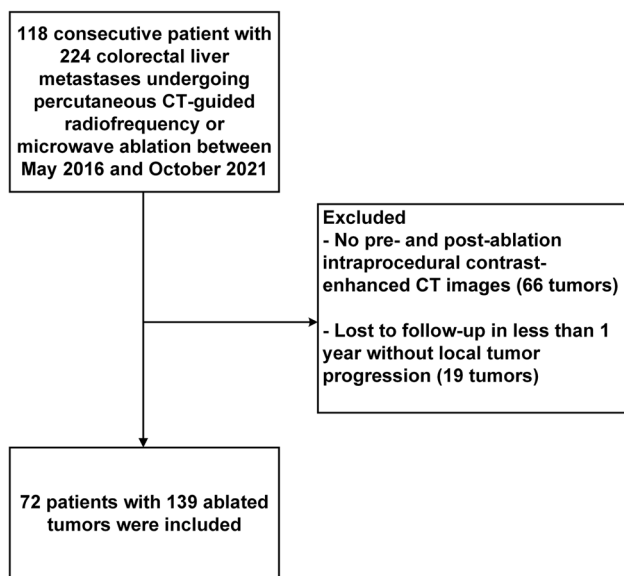
Materials and methods

Study population

We conducted a single-institution retrospective assessment of patients who underwent CT-guided microwave or radiofrequency ablation for CLM between May 2016 and October 2021. This assessment was performed using data from a liver ablation registry in a single institution (IRB No. PA-15–0566), which adhered to the Health Insurance Portability and Accountability Act and had a waiver of informed consent. In order to be eligible for percutaneous microwave or radiofrequency ablation, patients could have up to five CLMs, each measuring ≤ 5 cm, and no more than three extrahepatic sites of disease (e.g., pulmonary nodules, lymph nodes, or peritoneal nodules). Exclusion criteria for this study included patients who lacked both intraprocedural pre- and final post-ablation contrast-enhanced CT images, as well as tumors that were followed for less than 1 year without local tumor progression (LTP) (Fig. 1).

CT-guided ablation procedure and follow-up

All CT-guided percutaneous ablation procedures were carried out by board-certified interventional radiologists. The exact method of CT guided ablation has been previously described [6, 11]. The objective of all procedures

118 consecutive patient with 224 colorectal liver metastases undergoing percutaneous CT-guided radiofrequency or microwave ablation between May 2016 and October 2021

Excluded
- No pre- and post-ablation intraprocedural contrast-enhanced CT images (66 tumors)

- Lost to follow-up in less than 1 year without local tumor progression (19 tumors)

72 patients with 139 ablated tumors were included

Fig. 1 Participant flowchart

was to achieve ablative margins of ≥ 5 mm, which was assessed by comparing pre- and post-ablation contrast-enhanced CT images. This assessment was performed using a two-dimensional anatomic landmarks-based margin visual assessment method, a commercially available intensity-based ablation confirmation software (NEUWAVE™ System, NeuWave Medical), or an investigational ablation confirmation software currently undergoing clinical evaluation (ClinicalTrials.gov identifier: NCT04083378) [12].

Ablation outcomes were assessed according to reporting standards for ablation [13]. Post-ablation contrast-enhanced CT, MRI, or PET examinations were used to assess imaging-related local oncologic outcomes. Residual tumor and LTP definitions were applied accordingly to the criteria described by Ahmed et al [13]. For this particular study, two interventional radiologists (B.C.O. and Y.-M.L., with 14 and 6 years of experience, respectively) independently evaluated all available cross-sectional images. They were blinded to the results of MAM and their assessment determined the oncological outcomes of each ablated tumor. In the event of disagreements regarding the oncological outcomes, a consensus was reached.

Deformable and rigid registration and ablative margin quantification

The intraprocedural pre- and post-ablation contrast-enhanced CT images were uploaded to a radiation therapy treatment planning system, RayStation version 11B DTK (RaySearch Laboratories), for ablative margin quantification, which was developed in-house [10]. The CT images were acquired in the axial plane during the portal venous phase, with an in-plane image resolution ranging from 0.6–1.0 mm × 0.6–1.0 mm, and an image thickness of 3 mm.

Autosegmentation based on custom convolutional neural networks was performed on both the pre- and final post-ablation CT images to contour the liver, target tumor, and ablation zone [14, 15]. Subsequently, two different registration methods were employed to align the pre- and post-ablation CT images. The first method involved intensity-based RIR, utilizing gray-level cross-correlation of the liver contours [10]. The second method utilized a biomechanical DIR approach based on finite element modeling [16, 17], which has been integrated and validated in the treatment planning system.

Following the image registration processes, the target tumor was propagated from the pre-ablation CT images to the post-ablation CT images using the results obtained from the RIR and DIR methods, respectively. No additional adjustment of the registration was performed. The MAM was then computed as the shortest distance between the boundaries of the target tumor and the ablation zone on the post-ablation CT images. The MAM was defined as a nonnegative number, where a measurement of > 0 mm indicated complete overlap between the ablative margin and tumor contours. In cases where the MAM was less than 5 mm, a virtual 5-mm ablative margin was artificially created on the intraprocedural post-ablation CT images [6, 10]. The tissue not covered by the ablation zone within this virtual 5-mm margin was considered tissue at risk for tumor progression. For subcapsular (< 10 mm from the liver edge) or perivascular (< 10 mm from a vessel ≥ 3 mm in diameter) tumors, calculation of the MAM did not include the area abutting the liver capsule or adjacent vessel.

The registrations obtained from both methods were assessed to determine the geometric accuracy of the registration, following the recommendations outlined by the American Association of Physicists in Medicine Task Group 132 [18]. The alignment of the liver contour was evaluated using the Dice similarity coefficient (DSC) [19]. The DSC is calculated by multiplying the volume where the pre- and post-ablation liver contours overlap by 2 and dividing it by the total volume of both contours combined. As the contours converge and agree more closely, the DSC value approaches 1. Conversely, if the volumes diverge, resulting in two nonoverlapping structures, the DSC value approaches 0. Additionally, if the tumor, completely confined within the liver on the pre-ablation image, was found to be located outside the liver boundary after image registration, the volume of tumor

outside the liver was recorded as a metric of registration uncertainty.

Statistical analyses

Categorical data were presented as frequencies and percentages, while quantitative data were expressed as means ± SD or medians with interquartile range (IQR) when appropriate. The Wilcoxon signed-rank test was used to detect the difference in paired data and the Mann–Whitney U test was used for ordinal data. The measurement agreement of MAM of two registration methods was evaluated using the Bland–Altman analysis.

Table 1 Patient and tumor characteristics

Variable	Value
Patient characteristics	**N = 72**
Age ± SD (years)	57 ± 12
Gender	
Female	28 (39)
Male	44 (61)
Extrahepatic metastasis	39 (56)
CEA level (ng/mL)	
≤ 5	46 (66)
> 5	24 (34)
Tumor characteristics	**N = 139**
Mean tumor size ± SD (cm)	1.5 ± 0.8
Median tumor volume (interquartile range) (mL)	0.9 (0.4, 1.8)
Subcapsular tumor	86 (62%)
Perivascular tumor	28 (20%)
Use of intraprocedural ablation confirmation software	9 (6%)
Ablation modalities	
Radiofrequency	9 (6%)
Microwave	130 (94%)

Data are numbers of tumors with percentages, unless otherwise indicated

SD standard deviation, *CEA* carcinoembryonic antigen

To evaluate the factors associated with any difference of MAM measurement of two registration methods, univariable and multivariable logistic regression analyses were performed.

To evaluate the performance of MAM, generated by different registration methods, in predicting residual tumor and 1- and 2-year LTP, the area under the receiver operating characteristic curve (AUC) with 95% confidence intervals (CI) was calculated. Subgroup analyses were conducted using different tumor characteristics. The AUC values were compared using the DeLong method. Cumulative incidence functions were utilized to estimate the time to LTP, considering death a competing event. Competing-risks analysis, employing the Fine and Gray subdistribution hazard model, was employed to assess associations between time to LTP and clinical factors, including MAM. Statistical significance was determined with a threshold of p values less than 0.05. All calculations were performed on a per-tumor basis, and the statistical analyses were conducted using the R statistical software (version 4.2.3; The R Foundation).

Results

Study population

A total of 72 patients (mean age of 57 years ± 12 (SD), 44 men) and 139 ablated tumors (mean size of 1.5 cm ± 0.8 (SD)) were included. Patient and tumor characteristics are summarized in Table 1. Over a median follow-up period of 29.4 months (range, 11.7 to 74.0 months), residual tumor rate was 0.7% (1/139) and the LTP rate was 17.4% (24/138). The cumulative incidences of LTP at 12 and 24 months were 12% (95%CI 7, 18) and 14% (95%CI 9, 21), respectively.

Image registration and ablative margin quantification

Table 2 presents the results of the registration and ablative margin assessment. There was no significant difference between the median MAM quantified by the DIR and RIR methods. The mean MAM differences between the DIR and RIR methods were −0.2 mm, with a limit of

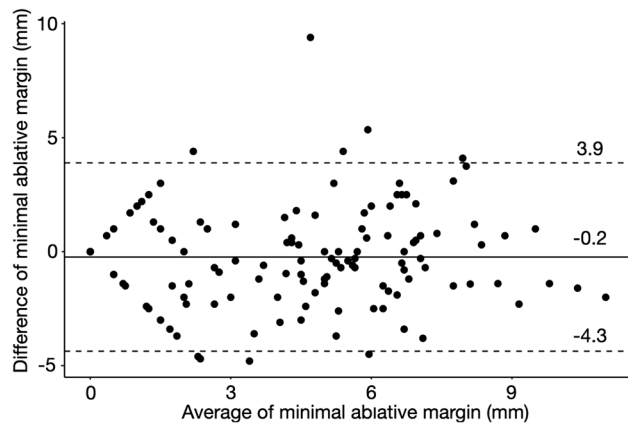**Table 2** Registration and minimal ablative margin assessment

Variables	Deformable registration	Rigid registration	*p* value
Dice similarity coefficient	0.97 (0.97, 0.98)	0.96 (0.93, 0.97)	< 0.001
Minimal ablative margin (mm)	4.7 (1.6, 6.0)	4.0 (1.0, 6.4)	0.08
Minimal ablative margin			0.2
0	28 (20%)	31 (22%)	
> 0 to < 5 mm	43 (31%)	51 (37%)	
≥ 5 to < 10 mm	64 (46%)	54 (39%)	
≥ 10 mm	4 (3%)	3 (2%)	
Volume of tissue at risk for progression (mL)	0.01 (0, 0.5)	0.05 (0, 0.6)	0.05

Data are numbers of tumors with percentages or median with interquartile range

Lin *et al. European Radiology* (2024) 34:5541–5550

5545

Table 3 Subgroup analyses of minimal ablative margin quantified by deformable and rigid registration methods stratified by subcapsular location, perivascular location, and tumor size

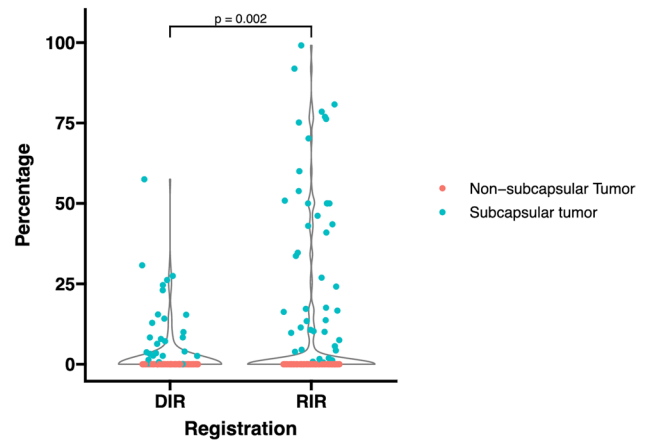| Variables	Subcapsular tumor ($n = 86$)	Non-subcapsular tumor ($n = 53$)	Perivascular tumor ($n = 28$)	Non-perivascular tumor ($n = 111$)	Size ≥ 2 cm ($n = 26$)	Size < 2 cm ($n = 113$)
Minimal ablative margin (deformable image registration)						
0	19 (22%)	9 (17%)	3 (11%)	25 (22%)	12 (46%)	16 (14%)
> 0 to < 5 mm	28 (33%)	15 (28%)	9 (32%)	34 (31%)	5 (19%)	38 (34%)
≥ 5 to < 10 mm	36 (42%)	28 (53%)	15 (53%)	49 (44%)	9 (35%)	55 (49%)
≥ 10 mm	3 (3%)	1 (2%)	1 (4%)	3 (3%)	0	4 (3%)
Minimal ablative margin (rigid image registration)						
0	21 (25%)	10 (19%)	2 (7%)	29 (26%)	11 (42%)	20 (18%)
> 0 to < 5 mm	30 (35%)	21 (40%)	12 (43%)	39 (35%)	7 (27%)	44 (39%)
≥ 5 to < 10 mm	33 (38%)	21 (40%)	13 (46%)	41 (37%)	7 (27%)	47 (41%)
≥ 10 mm	2 (2%)	1 (2%)	1 (4%)	2 (2%)	1 (4%)	2 (2%)

Data are numbers of tumors with percentages

Fig. 2 Bland–Altman plot of minimal ablative margin quantified by deformable versus rigid registration methods. The mean difference of minimal ablative margin was –0.2 mm, with an agreement between 3.9 and –4.3 mm


Fig. 3 Violin plot shows the percentages of each tumor volume mapped outside the liver with deformable versus rigid image registration methods ($p = 0.002$)

agreement ranging from 3.9 to –4.3 mm (Fig. 2). Subgroup analyses of MAM quantified by DIR versus RIR methods stratified by subcapsular location, perivascular location, and tumor size are demonstrated in Table 3.

The biomechanical DIR yielded a median liver DSC of 0.97 (range, 0.96–0.98), while the RIR resulted in a median DSC of 0.96 (range, 0.67–0.98) ($p < 0.001$). Only one patient had RIR DSC of < 0.80, who was re-positioned during the procedure. Out of 139 tumors, 27 (19%) were partially or totally mapped outside the liver using the DIR method, while there were 46 (33%) using the RIR method ($p < 0.001$). All of those tumors were subcapsular tumors. The median percentage of tumor volume mapped outside the liver was 0% (IQR [0, 0]) for DIR, and 0% (IQR [0, 7]) for RIR ($p = 0.002$) (Fig. 3). Figure 4 displays a representative case.

The univariable and multivariable logistic regression analyses showed tumor size and perivascular location were two independent factors in predicting any difference of MAM between the two registration methods (Table 4).

Local ablation outcomes and minimal ablative margin

The MAM in residual tumors and tumors with LTP ranged from 0 to 3.2 mm using the DIR method and from 0 to 7.6 mm using the RIR method. In terms of predicting residual tumor and 1-year LTP, the AUC was 0.89 (95%CI 0.83, 0.94) for the DIR method and 0.72 (95%CI 0.61, 0.83) for the RIR method ($p < 0.001$) (Fig. 5). Similarly, the DIR method had higher AUC than RIR in predicting 2-year LTP rates (90% versus
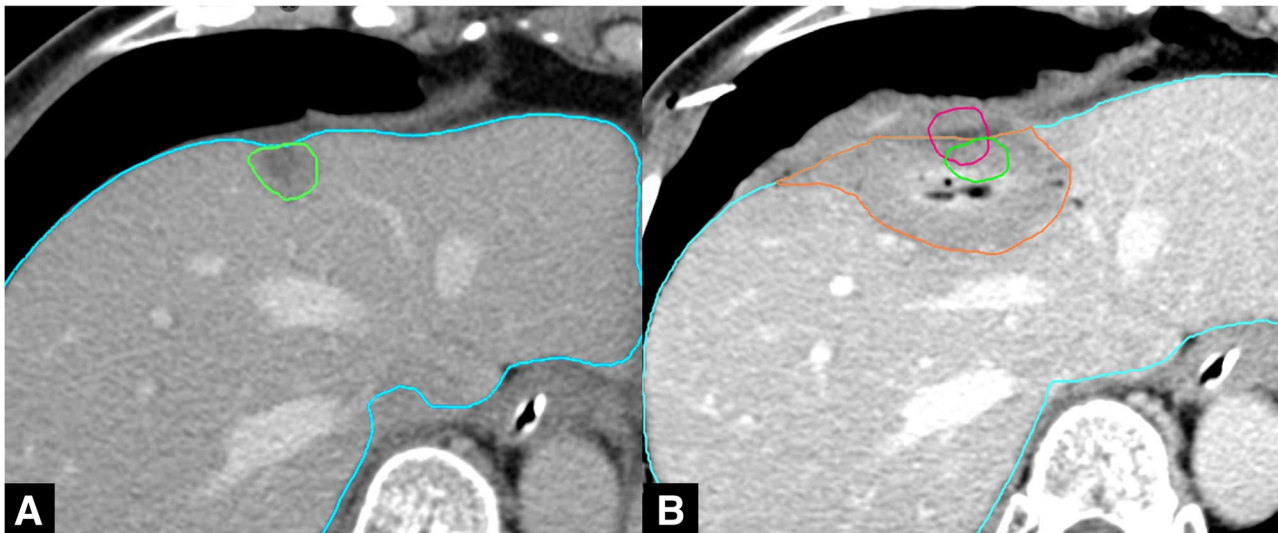
Fig. 4 Images of a 74-year-old woman who had one 1.7-cm colorectal liver metastasis undergoing CT-guided microwave ablation processed with minimal ablative margin quantification with deformable and rigid registration methods. **A** Axial contrast-enhanced CT scan obtained before ablation shows segmentation of liver (blue) and target tumor (green). **B** Axial contrast-enhanced CT scan obtained immediately after ablation with segmentation of liver (blue), ablation zone (orange), and mapped target tumor using deformable (green) and rigid (red) registration methods shows retraction of liver edge. The rigid registration method mapped the target tumor outside liver, which resulted in a falsely larger MAM quantification
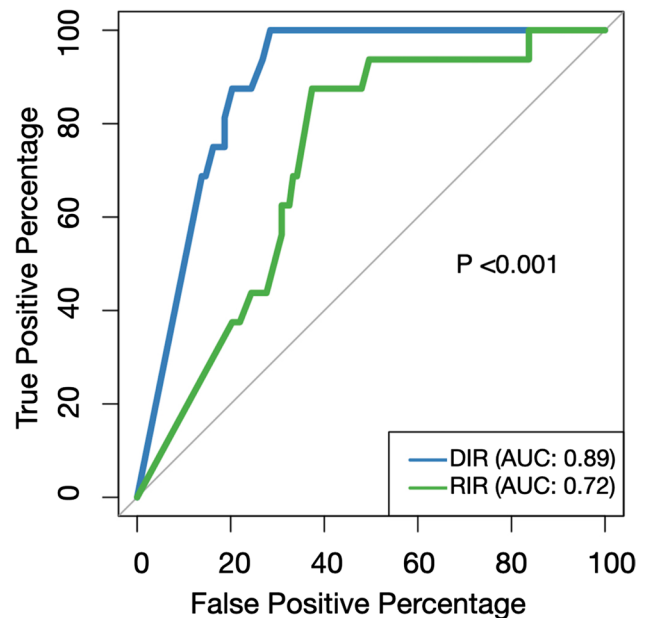
Table 4 Univariable and multivariable logistic regression of factors associated with any difference of minimal ablative margin between two registration methods

Variables	Univariable analysis		Multivariable analysis	
	Odds ratio	*p* value	Odds ratio	*p* value
Tumor size		0.02		0.02
< 2 cm	Reference		Reference	
≥ 2 cm	0.3 (0.1, 0.8)		0.3 (0.1, 0.8)	
Perivascular location	7.1 (1.4, 129.0)	0.01	6.5 (1.2, 122.0)	0.03
Subcapsular location	0.97 (0.4, 2.4)	0.94	1.4 (0.5, 3.7)	0.51
Volume of ablation zone (mL) (continuous)	1.0 (1.0, 1.01)	0.79	1.0 (1.0, 1.02)	0.59

Numbers in parentheses are 95%CIs

Fig. 5 Receiver operating characteristic curves for predicting residual tumor and 1-year local tumor progression by minimal ablative margin quantified by deformable versus rigid registration methods

72%; $p < 0.001$) (Supplementary Fig. S1). When tumors were stratified according to location and size, the AUC of predicting residual tumor and 1-year LTP was higher for the DIR method than the RIR method (Fig. 6).

In the univariable competing-risks regression model, tumor size, MAM, and the volume of tissue at risk for tumor progression were significant predictors of LTP. After adjusting for tumor size, an MAM of 0 quantified by DIR had the highest subdistribution hazard ratio (SHR) of 9.3 (95%CI 4.1, 20.8; $p < 0.001$) (Table 5).

Lin *et al. European Radiology* (2024) 34:5541–5550

5547
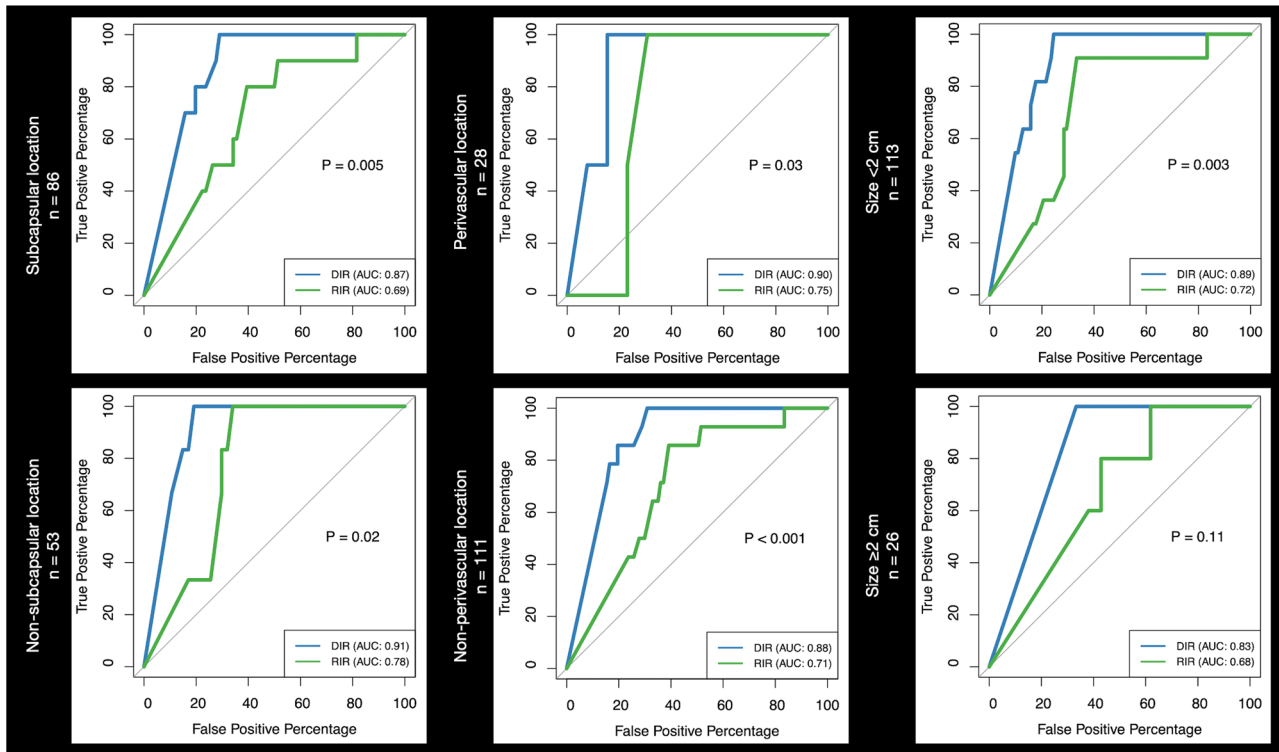
Fig. 6 Subgroup analyses of receiver operating characteristic curves for predicting residual tumor and 1-year local tumor progression by minimal ablative margin quantified by deformable versus rigid registration methods stratified by subcapsular location (left column), perivascular location (middle column), and tumor size (right column)

Table 5 Subdistribution hazard ratio for factors associated with local tumor progression by competing-risks regression model

Variables	Subdistribution hazard ratio	*p* value	Adjusted subdistribution hazard ratio	*p* value
Deformable image registration				
Minimal ablative margin (mm)		< 0.001		< 0.001
> 0 (*n* = 111)	Reference		Reference	
0 (*n* = 28)	10.0 (4.4, 22.5)		9.3 (4.1, 20.8)	
Volume of tissue at risk for tumor progression (mL) (continuous)	1.5 (1.2, 1.8)	< 0.001	1.4 (1.1, 1.8)	0.004
Rigid image registration				
Minimal ablative margin (mm)		0.02		0.03
> 0 (*n* = 108)	Reference			
0 (*n* = 31)	2.7 (1.2, 5.9)		2.4 (1.1, 5.2)	
Volume of tissue at risk for tumor progression (mL) (continuous)	1.1 (0.98, 1.3)	0.1	1.1 (0.9, 1.2)	0.37

Numbers in parentheses are 95%CIs

Discussion

Accurate and reproducible image registration methods are prerequisites for ablation confirmation software in evaluating ablation completeness. In this study, we found that using biomechanical deformable image registration (DIR) for minimal ablative margin (MAM) quantification was more accurate in liver registration and outperformed the intensity-based rigid image registration (RIR) method in predicting local tumor outcomes in patients with colorectal liver metastasis (CLM) undergoing thermal ablation. This was demonstrated by a higher area under the receiver operating characteristic curve (AUC) (0.90 versus

5548

Lin *et al. European Radiology* (2024) 34:5541–5550

0.72; $p < 0.001$) and subdistribution hazard ratio (SHR) (9.3 versus 2.4), regardless of tumor size and location.

Excellent registration accuracy and short processing time are crucial when utilizing ablation confirmation software during clinical ablation procedures [18]. Quick and accurate decisions regarding the necessity of immediate repeated ablation are of utmost importance in such cases. While RIR offers advantages of simple implementation and fast processing, our present study demonstrates that DIR outperformed the RIR method in terms of Dice similarity coefficient (DSC). The DIR method yielded the excellent lowest DSC of 0.96, whereas the RIR method produced the lowest DSC of 0.67, even in CT images acquired using the same scanner and settings within the same procedure. The patient with RIR DSC of 0.67 had a change in positioning during the procedure. According to the American Association of Physicists in Medicine Task Group 132 [18], a DSC range of 0.80 to 0.90 is considered acceptable. This is especially valuable considering that registration of two CT image sets collected at different times can be challenging due to different image levels or deformation of the liver caused by the patient's breathing, heartbeat, or tissue retraction following ablation, change of position on the CT table, etc. Restricting the registration of two images to simple rigid transformations often leads to remaining uncertainties due to the deformable nature of soft tissue. Although DIR holds potential for mitigating these uncertainties, limitations and challenges persist. In present study, we observed that several subcapsular tumors were partially mapped outside the liver contour, even when the biomechanical DIR method was employed. The DIR algorithm employs a deformation model, which can be over-constrained in some circumstances. For instance, DIR algorithms assume smoothness of the vector field created on liver contours. However, this assumption may result in registration errors when a singularity in the vector field exists with significant local deformation. The large number of degrees of freedom in DIR can also lead to ambiguity in the deformation vector field for certain algorithms, particularly in areas with unsmooth contours. Consequently, registration in these unsmooth areas can be prone to inaccuracies. Nevertheless, in this study, fewer tumors were observed mapped partially outside the liver using the DIR method than the RIR method (19% versus 33%, $p < 0.001$) and the interquartile range of the volume mapped outside of the liver was smaller for the DIR method than the RIR method ([0,0] versus [0,7], $p = 0.002$).

Numerous studies have demonstrated that three-dimensional ablation confirmation software outperforms visual comparison of pre- and post-ablation two-dimensional CT images [7–9]. However, notable limitations in image registration have been observed. In these studies,

patient selection was crucial to minimize registration errors, necessitating the inclusion of patients with similar image characteristics, such as slice thickness, image number, and position. Manual adjustments to image registration were also required in these studies. For instance, a study using rigid registration for ablative margin assessment found 14% of tumors failed at image registration [7]. Another study evaluating ablation confirmation software using intensity-based DIR method reported manual adjustment in 24% of cases [9]. Similarly, two other studies utilizing different registration methods had to exclude 14–16% of cases due to failed registration [7, 20]. In two commercially available ablation confirmation software, additional measurements were necessary to quantify ablative margins in subcapsular regions [8, 9]. These image registration failures limited the use of ablation confirmation software, particularly when deformations occurred during the ablation, such as artificial ascites and liver tissue contraction following ablation.

In our study, biomechanical DIR achieved good accuracy without the need for adjustments. Only 19% (27/139) of tumors were partially or totally mapped outside the liver when DIR method was applied. We believe this is attributable to radical changes in the liver contour resulting from the contraction and dehydration of the ablation zone following the ablation. The DIR algorithm assumes smoothness of the liver contours and leads to registration error in these cases. However, it is arguable that the volume of the ablated tumor was reduced following ablation as well. However, this phenomenon was not reflected in this model. Therefore, the assumed smoothness of the controlled liver contour by the algorithm caused the target tumor to be partially mapped outside the actual liver contour, mimicking the shrinkage of the ablated tumor and providing a corrected ablative margin. Lastly, it is worth noting that biomechanical DIR errors were less frequent in our present study compared to the rigid method. In a total of 86 subcapsular tumors, only 27 (31%) had this phenomenon when DIR was used, compared to 46 (53%) when RIR was used. Further, previous research has shown that biomechanical DIR is more accurate than other DIR methods in liver images [10, 21–24]. If RIR is used to quantify the ablative margin of subcapsular tumors, caution should be exercised to account for potential registration errors. In this study, we found that smaller tumors and perivascular tumors were associated with larger differences in MAM quantified by DIR and RIR methods. However, this might be explained by the fact that more tumors with a MAM of 0 mm were observed in larger or non-perivascular tumors, which contributed to a smaller influence of registration methods on MAM quantification. These findings did not translate into clinical outcomes when subgroup

Lin *et al. European Radiology* (2024) 34:5541–5550

5549

analyses with stratifications of tumor size and location were applied, which supported using DIR method in any circumstances.

One limitation of this study is its retrospective design conducted within a single institution. At our institution, liver ablation procedures were performed under CT guidance. However, the decision to acquire intraprocedural contrast-enhanced CT scans was at the discretion of the operators. In our cohort, up to 30% of cases did not have complete pre- and post-ablation contrast-enhanced CT images and had to be excluded. This exclusion may introduce a selection bias, potentially limiting the generalizability of our findings. Moreover, concerns regarding contrast-induced nephropathy following contrast-enhanced CT scans may limit its use. Furthermore, we did not compare the biomechanical DIR method with other available ablation software that employ different DIR methods. This comparison is an area that warrants further investigation. Additionally, we did not subjectively assess the accuracy of registration through visual inspection of anatomical landmarks, as it is subjective and susceptible to errors associated with two-dimensional image comparison. A study proposing the use of vessel bifurcation detection in CT scans for automatic and objective assessment of DIR accuracy has been put forth [25].

In conclusion, this study supports the role of biomechanical deformable image registration (DIR) as the preferred image registration method over rigid image registration (RIR) for quantifying minimal ablative margin (MAM) using intraprocedural contrast-enhanced CT images. Therefore, we recommend utilizing biomechanical DIR for ablative margin quantification whenever feasible. However, caution must be exercised when dealing with subcapsular tumors that involve significant liver edge contraction, as complex deformations of this nature may not be effectively addressed by any of the available registration methods.

Abbreviations

AUC   Area under the receiver operating characteristic curve
CI   Confidence interval
CLM   Colorectal liver metastasis
DIR   Deformable image registration
LTP   Local tumor progression
MAM   Minimal ablative margin
RIR   Rigid image registration

Supplementary Information

The online version contains supplementary material available at https://doi.org/10.1007/s00330-024-10632-8.

> Below is the link to the electronic supplementary material. Supplementary file1 (PDF 79 KB)

Declarations

Guarantor
The scientific guarantor of this publication is Dr. Bruno C. Odisio.

Conflict of interest
Kristy K.Brock: Grants from the National Institutes of Health and RaySearch Laboratories; licensing agreement with RaySearch Laboratories; travel support from The American Association of Physicists in Medicine; patents planned, issued, or pending; advisory board, RaySearch Laboratories.
Bruno C.Odisio: Research grants from Siemens Healthineers and Johnson & Johnson; consulting fees from Siemens Healthineers.

Statistics and biometry
One of the authors (Iwan Paolucci) has significant statistical expertise.

Informed consent
Written informed consent was waived by the Institutional Review Board.

Ethical approval
Institutional Review Board approval was obtained.

Study subjects or cohorts overlap
Forty patients (29%) in the current study cohort overlap with a previous study reported in *Radiology* (doi: https://doi.org/10.1148/radiol.221373).

Methodology

- retrospective
- observational
- performed at one institution

Author details
[1]Department of Interventional Radiology, The University of Texas MD Anderson Cancer Center, 1515 Holcombe Blvd, Houston, TX 77030, USA. [2]Department of Imaging Physics, The University of Texas MD Anderson Cancer Center, 1515 Holcombe Blvd, Houston, TX 77030, USA.

References

1. Engstrand J, Nilsson H, Strömberg C, Jonas E, Freedman J (2018) Colorectal cancer liver metastases - a population-based study on incidence, management and survival. BMC Cancer 18(1):78
2. Kow AWC (2019) Hepatic metastasis from colorectal cancer. J Gastrointest Oncol 10(6):1274–1298
3. Cervantes A, Adam R, Rosello S et al (2023) Metastatic colorectal cancer: ESMO Clinical Practice Guideline for diagnosis, treatment and follow-up. Ann Oncol 34(1):10–32
4. Lin YM, Paolucci I, Brock KK, Odisio BC (2021) Image-guided ablation for colorectal liver metastasis: principles, current evidence, and the path forward. Cancers (Basel) 13(16):3926
5. Tinguely P, Ruiter SJS, Engstrand J et al (2023) A prospective multicentre trial on survival after Microwave Ablation VErsus Resection for Resectable Colorectal liver metastases (MAVERRIC). Eur J Cancer 187:65–76
6. Lin YM, Paolucci I, O'Connor CS et al (2023) Ablative margins of colorectal liver metastases using deformable CT image registration and autosegmentation. Radiology 307(2):e221373
7. Kaye EA, Cornelis FH, Petre EN et al (2019) Volumetric 3D assessment of ablation zones after thermal ablation of colorectal liver

metastases to improve prediction of local tumor progression. Eur Radiol 29(5):2698–2705

8. Laimer G, Jaschke N, Schullian P et al (2021) Volumetric assessment of the periablational safety margin after thermal ablation of colorectal liver metastases. Eur Radiol 31(9):6489–6499

9. Vasiniotis Kamarinos N, Gonen M et al (2022) 3D margin assessment predicts local tumor progression after ablation of colorectal cancer liver metastases. Int J Hyperthermia 39(1):880–887

10. Anderson BM, Lin YM, Lin EY et al (2021) A novel use of biomechanical model-based deformable image registration (DIR) for assessing colorectal liver metastases ablation outcomes. Med Phys 48(10):6226–6236

11. Paolucci I, Lin YM, Jones AK, Brock KK, Odisio BC (2023) Use of contrast media during CT-guided thermal ablation of colorectal liver metastasis for procedure planning is associated with improved immediate outcomes. Cardiovasc Intervent Radiol 46(3):327–336

12. Lin YM, Paolucci I, Anderson BM et al (2022) Study protocol COVER-ALL: clinical impact of a volumetric image method for confirming tumour coverage with ablation on patients with malignant liver lesions. Cardiovasc Intervent Radiol 45(12):1860–1867

13. Ahmed M, Solbiati L, Brace CL et al (2014) Image-guided tumor ablation: standardization of terminology and reporting criteria–a 10-year update. Radiology 273(1):241–260

14. Anderson BM, Rigaud B, Lin YM et al (2022) Automated segmentation of colorectal liver metastasis and liver ablation on contrast-enhanced CT images. Front Oncol 12:886517

15. Anderson BM, Lin EY, Cardenas CE et al (2021) Automated contouring of contrast and noncontrast computed tomography liver images with fully convolutional networks. Adv Radiat Oncol 6(1):100464

16. Brock KK, Sharpe MB, Dawson LA, Kim SM, Jaffray DA (2005) Accuracy of finite element model-based multi-organ deformable image registration. Med Phys 32(6):1647–1659

17. Velec M, Moseley JL, Svensson S, Hardemark B, Jaffray DA, Brock KK (2017) Validation of biomechanical deformable image registration in the abdomen, thorax, and pelvis in a commercial radiotherapy treatment planning system. Med Phys 44(7):3407–3417

18. Brock KK, Mutic S, McNutt TR, Li H, Kessler ML (2017) Use of image registration and fusion algorithms and techniques in radiotherapy: report of

the AAPM Radiation Therapy Committee Task Group No. 132. Med Phys. 44(7):e43–e76

19. Dice LR (1945) Measures of the amount of ecologic association between species. Ecology 26(3):297–302

20. Ruiter SJS, Tinguely P, Paolucci I et al (2021) 3D quantitative ablation margins for prediction of ablation site recurrence after stereotactic image-guided microwave ablation of colorectal liver metastases: a multicenter study. Front Oncol 11:757167

21. Brock KK, Dawson LA, Sharpe MB, Moseley DJ, Jaffray DA (2006) Feasibility of a novel deformable image registration technique to facilitate classification, targeting, and monitoring of tumor and normal tissue. Int J Radiat Oncol Biol Phys 64(4):1245–1254

22. Velec M, Moseley JL, Eccles CL et al (2011) Effect of breathing motion on radiotherapy dose accumulation in the abdomen using deformable registration. Int J Radiat Oncol Biol Phys 80(1):265–272

23. Kuznetsova S, Grendarova P, Roy S, Sinha R, Thind K, Ploquin N (2019) Structure guided deformable image registration for treatment planning CT and post stereotactic body radiation therapy (SBRT) Primovist((R)) (Gd-EOB-DTPA) enhanced MRI. J Appl Clin Med Phys 20(12):109–118

24. Sen A, Anderson BM, Cazoulat G et al (2020) Accuracy of deformable image registration techniques for alignment of longitudinal cholangiocarcinoma CT images. Med Phys 47(4):1670–1679

25. Cazoulat G, Anderson BM, McCulloch MM, Rigaud B, Koay EJ, Brock KK (2021) Detection of vessel bifurcations in CT scans for automatic objective assessment of deformable image registration accuracy. Med Phys 48(10):5935–5946

Publisher's Note